

1 **Title:** A simple model for determining affinity from irreversible thermal shifts

2

3 **Author:** Justin Hall

4

5 **Supplemental Information**

6 **Extended derivations**

7  $\Delta G_L = -RT \ln(Q)$  (1)

8  $\therefore Q = \frac{[F]}{[F]} + \frac{[FL]}{[F]} = 1 + \frac{[L]}{K_D}$

9  $\Delta G_L = RT \ln\left(1 + \frac{[L]}{K_D}\right)$  (2)

10 where  $T$  is in Kelvin, and is fixed at the temperature at which the KD was determined (eg, 298 K).

11  $\Delta^L G_u - \Delta G_u = \Delta^u G_L - \Delta G_L$  (3)

12  $k = A e^{-Ea_1/RT}$  (4)

13  $Ea = \Delta G + \Delta G_{\ddagger}^{\ddagger}$  (5)

14  $A_1 \cong A_2$  (6)

15  $\Delta TM = TM_{,bound} - TM_{,apo}$  (7)

16  $k_{U1} = A_1 e^{\left(\frac{-Ea_1}{RT_{m,apo}}\right)}$  (8)

17  $k_{U2} = A_2 e^{\left(\frac{-Ea_2}{R(T_{m,apo} + \Delta Tm)}\right)}$  (9)

18  $\therefore k_{U1}$  at  $TM_{,apo}$  is approximately equal to  $k_{U2}$  at  $TM_{,bound}$  (see equations (25-28), **SI Fig. 1** and

19 **SI Fig 2)**

20  $I = \frac{k_{U1}}{k_{U2}} = \frac{A_1}{A_2} \frac{e^{\left(\frac{-Ea_1}{RT_{m,apo}}\right)}}{e^{\left(\frac{-Ea_2}{R(T_{m,apo} + \Delta Tm)}\right)}} = e^{\left(\frac{Ea_2}{R(T_{m,apo} + \Delta Tm)}\right) - \left(\frac{Ea_1}{RT_{m,apo}}\right)}$  (10)

21  $\therefore \ln(e^{(x)}) = x \quad \text{and} \quad \ln(1) = 0$

$$22 \quad \frac{Ea_2}{R(Tm_{apo} + \Delta Tm)} = \frac{Ea_1}{RTm_{apo}} \quad (11)$$

$$23 \quad Ea_2 = \frac{Ea_1 R(Tm_{apo} + \Delta Tm)}{RTm_{apo}} = Ea_1 \left( 1 + \frac{\Delta Tm}{Tm_{apo}} \right) = Ea_1 + Ea_1 \left( \frac{\Delta Tm}{Tm_{apo}} \right) \quad (12)$$

$$24 \quad \Delta G_U = Ea_1 - \Delta G_{U\dagger} \quad (13)$$

$$25 \quad \Delta^L G_U = Ea_2 - \Delta^L G_{U\dagger} \quad (14)$$

26 Substitute equation (13) and (14) into equation (3):

$$27 \quad (Ea_2 - \Delta^L G_{U\dagger}) - (Ea_1 - \Delta G_{U\dagger}) = \Delta^U G_L - \Delta G_L \quad (15)$$

28 Substitute equation (12) into equation (15) and simplify:

$$29 \quad Ea_1 \left( \frac{\Delta Tm}{Tm_{apo}} \right) + \Delta G_{U\dagger} - \Delta^L G_{U\dagger} = \Delta^U G_L - \Delta G_L \quad (16)$$

$$30 \quad \Delta G_{U\dagger} \cong \Delta^L G_{U\dagger} \quad (17)$$

$$31 \quad Ea_1 \left( \frac{\Delta Tm}{Tm_{apo}} \right) = \Delta^U G_L - \Delta G_L \quad (18)$$

32 Since ligand does not bind to unfolded protein:

$$33 \quad Ea_1 \left( \frac{\Delta Tm}{Tm_{apo}} \right) = -\Delta G_L \quad (19)$$

34 Substitute equation (2) into equation (19), followed by rearrangement gives:

$$35 \quad -RT \ln \left( 1 + \frac{[L]}{K_D} \right) = RT \ln \left( \frac{K_D}{K_D + [L]} \right) = -Ea_1 \left( \frac{\Delta Tm}{Tm_{apo}} \right) \quad (20)$$

36 Experimentally, the apparent  $\Delta Tm$  ( $\Delta Tm_{APP}$ ), will be the sum of the ligand binding to the site of

37 interest ( $\Delta Tm$ ), plus any additional extra-site binding ( $\Delta Tm_X$ ):

38  $\Delta T_{M,APP} = \Delta T_M + \Delta T_{M_X}$  (21)

39 Combining equations (20) and (21) we find:

40  $\Delta T_{M,APP} = -\left(\frac{T_{m,apo}RT}{Ea_1}\right) \ln\left(\frac{K_{D,app}}{K_{D,app}+[L]}\right) = -\left(\frac{T_{m,apo}RT}{Ea_1}\right) \left(\ln\left(\frac{K_D}{K_D+[L]}\right) + \ln\left(\frac{K_{Dx}}{K_{Dx}+[L]}\right)\right)$  (22)

41 where  $K_{D,APP}$  is the apparent affinity, and  $K_{Dx}$  is the affinity of extra-site binding. After  
42 rearrangement and simplification we find:

43  $\ln\left(\frac{K_D}{K_D+[L]}\right) = -\left(\frac{Ea_1}{RT}\right) \left(\frac{\Delta T_{M,APP}}{T_{m,apo}}\right) - \ln\left(\frac{K_{Dx}}{K_{Dx}+[L]}\right)$  (23)

44 where  $T$  is the temperature at which the  $K_D$  was determined (eg, 298 K).

45  $\therefore \ln\left(\frac{K_D}{K_D+[L]}\right) \cong \ln\left(\frac{K_D}{[L]}\right)$  when  $[L] \gg K_D$

46  $\ln\left(\frac{K_D}{[L]}\right) = -\left(\frac{Ea_1}{RT}\right) \left(\frac{\Delta T_{M,APP}}{T_{m,apo}}\right) - \ln\left(\frac{K_{Dx}}{K_{Dx}+[L]}\right)$  (24)

47

48 **Extended derivations for value of  $k_{U1}$  at  $T_{M,apo}$  and  $k_{U2}$  at  $T_{M,bound}$**

49 Beginning at equation (10), without assuming the ratio of the unfolding rate constants of apo and  
50 bound is unity,  $\frac{k_{U1}}{k_{U2}} = 1$ , substitution with equation (7) will yield:

51  $\frac{Ea_2}{RT_{m,bound}} = \frac{Ea_1}{RT_{m,apo}} + \ln\left(\frac{k_{U1}}{k_{U2}}\right)$  (25)

52 Rearrangement of equation (25) gives:

53  $Ea_2 = \frac{Ea_1 T_{m,bound}}{T_{m,apo}} + RT_{m,bound} \ln\left(\frac{k_{U1}}{k_{U2}}\right)$  (26)

54 From Sanchez-Ruiz *et al.* (Sanchez-Ruiz et al. 1988) we get the equivalence:

$$55 \frac{vEa_1}{RTm_{apo}^2} = kU_1 = A_1 e^{-Ea_1/RTm_{apo}} \quad (27)$$

56 where  $v$  is the heating rate of the irreversible unfolding experiment. If the apo and the bound  
 57 experiments are collected at the same heating rate, and  $A_1 \cong A_2$ , the ratio of the rate constants at  
 58 their TM temperatures is:

$$59 \frac{k_{u1}}{k_{u2}} = \frac{\left(\frac{Ea_1}{RTm_{apo}^2}\right)}{\left(\frac{Ea_2}{RTm_{bound}^2}\right)} = \frac{\left(\frac{Ea_1}{RTm_{apo}^2}\right)}{\left(\frac{Ea_1 Tm_{bound} + RTm_{bound} \ln\left(\frac{k_{u1}}{k_{u2}}\right)}{RTm_{bound}^2}\right)} = \frac{Ea_1 Tm_{bound}}{Ea_1 Tm_{apo} + RTm_{apo}^2 \ln\left(\frac{k_{u1}}{k_{u2}}\right)} \quad (28)$$

60 At the condition of  $TM_{apo} = TM_{bound}$ ,  $\Delta TM = 0$ ,  $\frac{k_{u1}}{k_{u2}} = 1$ , therefore  $\ln\left(\frac{k_{u1}}{k_{u2}}\right) = 0$ . Starting at  $\Delta TM = 0$ ,  
 61 steps can be taken through a range of  $\Delta TM$  values using an estimate of  $\ln\left(\frac{k_{u1}}{k_{u2}}\right)$  from the prior  $\Delta TM$   
 62 step (*eg*, to approximate  $\frac{k_{u1}}{k_{u2}}$  at  $\Delta TM = 1$ , the  $\ln\left(\frac{k_{u1}}{k_{u2}}\right)$  value from  $\Delta TM = 0$  is used). In this way it can  
 63 be demonstrated that under typical protein unfolding conditions (*eg*, TM between 50-70 °C),  $kU_1$   
 64 at  $TM_{apo}$  is approximately equal to  $kU_2$  at  $TM_{bound}$  (**SI Fig 1**). Similarly, using a numerical  
 65 integration approach, a simulation of unfolding can be made which also shows  $kU_1$  at  $TM_{apo}$  is  
 66 approximately equal to  $kU_2$  at  $TM_{bound}$  (**SI Fig 2**). Please note that since refolding is negligible in  
 67 this model, the rates constants of folding are not considered; if you have been reading this  
 68 extension of the derivation as a loop-out from the main or supplemental text assertion of rate  
 69 equivalence of  $kU_1$  at  $TM_{apo}$  and  $kU_2$  at  $TM_{bound}$ , you may now return to the rest of the derivation.

70

71 **Extended discussion on simulations**

72 In our laboratory experiments, we observed a ligand-dependent  $\Delta T_M$  shift beyond what  
73 can be explained by initial occupancy. One possibility is that the effect is due to unfolding through  
74 the apo unfolding pathway, which favors net ligand dissociation; thus, the ligand-dependent  $\Delta T_M$   
75 is due to kinetic competition between ligand rebinding to apo protein and unfolding through the  
76 apo path. To test this hypothesis, the simulation was adjusted to allow us to predict what  $\Delta T_M$   
77 results for the system when we have high initial occupancy of the bound form ( $\geq 90\%$ ), and then  
78 allow the system to evolve over time as the temperature increases. When no interconversion of  
79 apo and bound is allowed, we see a  $\Delta T_M$  that is the average of  $T_{M,apo}$  and  $T_{M,bound}$  values weighted  
80 by the initial proportions of apo and bound protein. This model represents the extreme of a very  
81 fast rate of rebinding or a very slow rate of dissociation, where no ligand-bound protein is ever  
82 lost to the apo unfolding pathway; we see that this system is saturable as the limit of 100-percent  
83  $T_{M,bound}$ , after which further ligand addition has no effect on  $\Delta T_M$ .

84 In contrast, a model that allows instantaneous transfer between the bound form to apo, but  
85 no transfer of apo to the bound state (unidirectional replacement of every molecule of apo that  
86 unfolds with a molecule of bound), represents the limit of very fast dissociation with very slow  
87 rebinding; this is the most aggressive example of a system where no ligand rebinding is allowed  
88 to protect the protein from unfolding beyond the initial equilibrium distribution of bound protein.  
89 As with the prior model, we see a system that is strongly influenced by the initial occupancy but  
90 even this extreme has only a slightly reduced apparent  $\Delta T_M$  compared to the  $\Delta T_M$  of the fast  
91 rebinding model (**SI Fig. 3**).

92 As can be seen in **SI Fig 3**, slow rebinding predicts a  $\Delta T_M$  that is very close to the first  
93 model as the initial occupancy approaches 100-percent bound. Therefore, both these models lack  
94 the non-saturable effect seen in experiments for increasing ligand concentration, suggesting this

95 phenomenon is not due to rate competition between ligand binding and the apo unfolding pathway  
96 for irreversible unfolding.

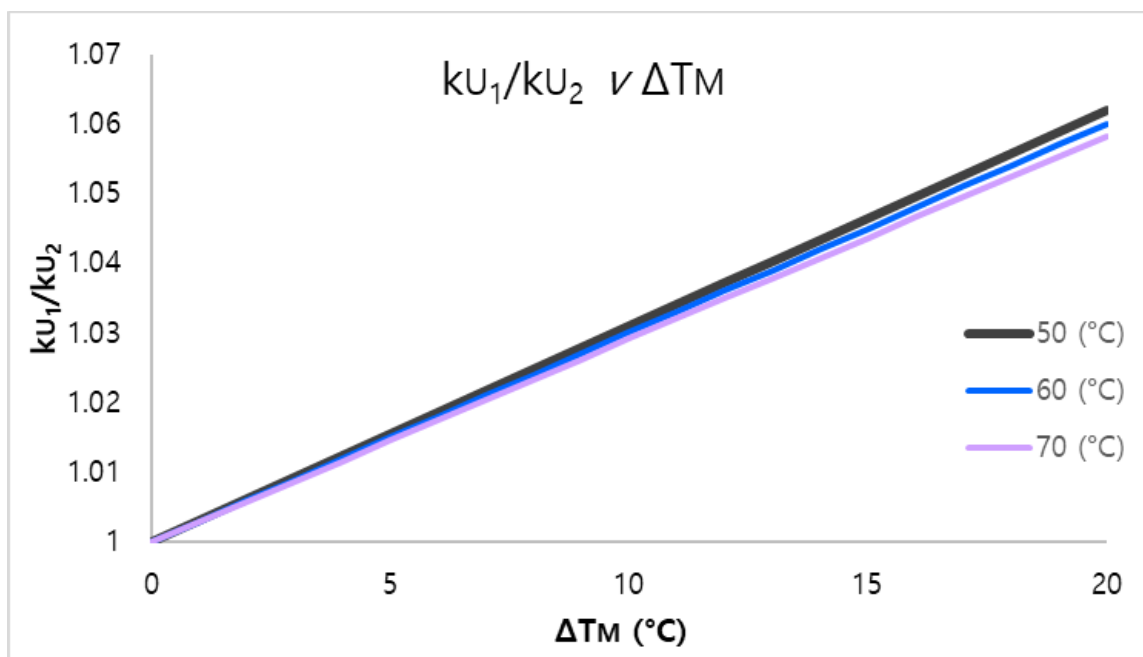
97         Lastly, these models begins with the equilibrium state, which then evolves with time and  
98 temperature. Based on these models, the initial equilibrium occupancy of the system seems to have  
99 a dominant influence on the final  $\Delta T_M$ . Inspection shows this is because  $\Delta T_M$  is equally dependent  
100 on the rate constants and the ligand occupancy (*eg*,  $k_{U_2} \times [FL]$ ); since the fold-change between the  
101 rate constants  $k_{U_1}$  and  $k_{U_2}$  at the same temperatures is small (*ca* 4-fold) (**SI Fig. 2**) compared to  
102 the fold-change in the concentration of apo and bound at 95-percent occupancy (*ca* 19-fold), most  
103 of the information for the resultant  $\Delta T_M$  is contained in the initial occupancy term.

104 **References**

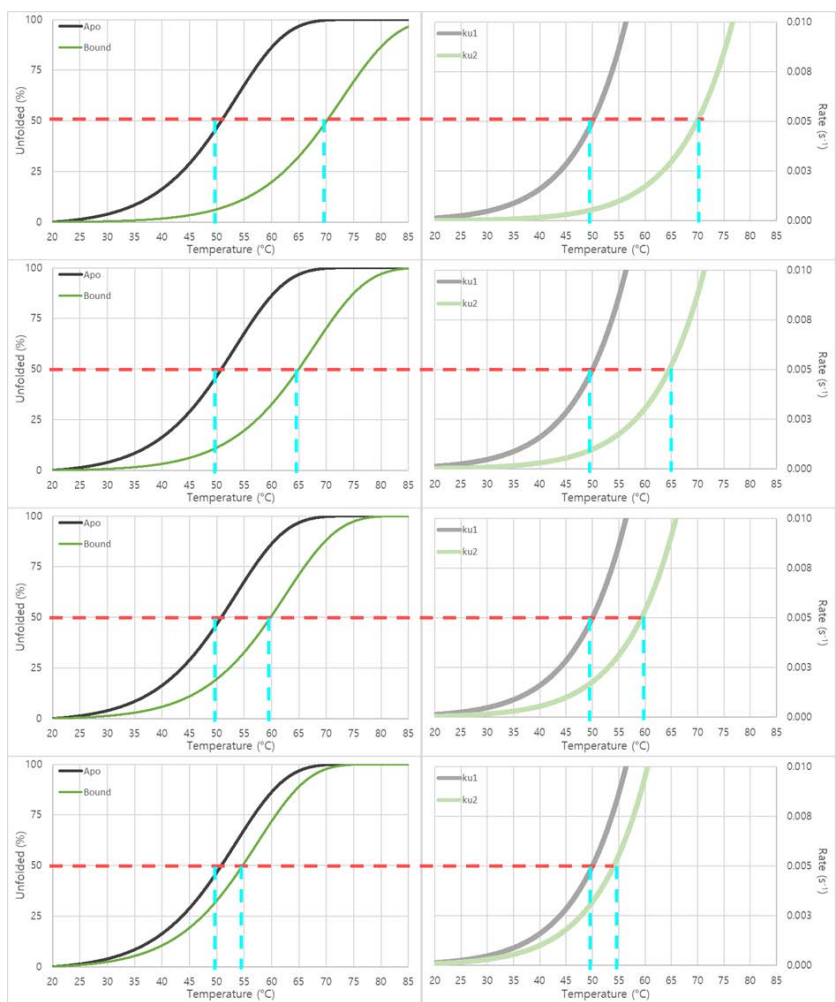
105 Sanchez-Ruiz, J. M., J. L. Lopez-Lacomba, M. Cortijo, and P. L. Mateo. 1988. 'Differential scanning  
106 calorimetry of the irreversible thermal denaturation of thermolysin', *Biochemistry*, 27: 1648-52.

107



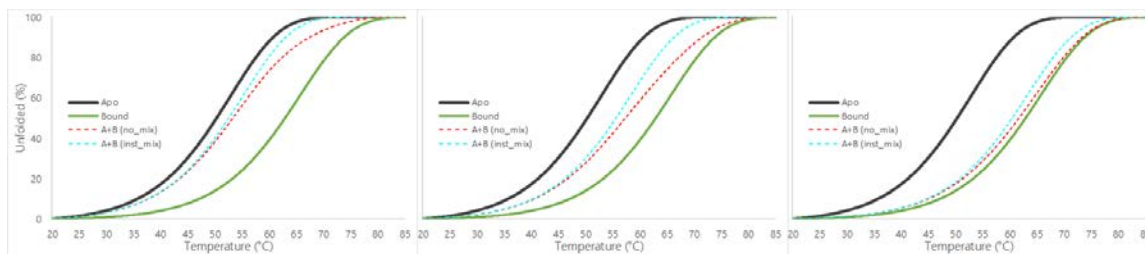


108  
 109 **SI Fig 1.** The value of the apo unfolding rate constant,  $kU_1$ , at  $T_{M,apo}$  divided by the value of the  
 110 bound unfolding rate constant,  $kU_2$ , at  $T_{M,bound}$ . For a two-state unfolding process, with unfolding  
 111 rates for apo ( $kU_1$ ) and bound ( $kU_2$ ) that are Arrhenius functions, where  $A_1 \cong A_2$ , the value of  $kU_1$   
 112 at  $T_{M,apo}$  is approximately the same value as  $kU_2$  at  $T_{M,bound}$ . Data were generated using equation  
 113 (28), with  $T_{M,apo}$  values of 50, 60 and 70 °C (vantablack, ultramarine and porphyry).



114

115 **SI Fig 2.** Simulated data showing unfolding and rate of unfolding. These data show that for a two-  
 116 state unfolding process, with unfolding rates for apo ( $ku_1$ ) and bound ( $ku_2$ ) that are Arrhenius  
 117 functions, where  $A_1 \cong A_2$ , the value of  $ku_1$  at  $T_{M,apo}$  is approximately the same value as  $ku_2$  at  
 118  $T_{M,bound}$ . Apo (black) and bound (green) unfolding profiles (left) or rate constant traces (right) are  
 119 shown; red and cyan dashed lines have been added to guide the eye. Unfolding data were modeled  
 120 using the methods described in equations (20-22) of the main text, with a data integration steps of  
 121 0.1 s, a ligand concentration of 100  $\mu\text{M}$ , and  $K_D$  values of 0.005, 0.05, 0.5 and 5  $\mu\text{M}$  (top to  
 122 bottom).



123  
 124 **SI Fig 3.** Simulations showing the  $T_M$  expected for 30 (left), 60 (middle) or 90-percent (right)  
 125 initial occupancy when there is very fast rebinding (red line) or very slow rebinding (cyan line)  
 126 relative to the apo unfolding rate. 100-percent apo (black) or bound (green) unfolding traces are  
 127 shown as reference. Data are for a heating rate of 4 °C/min. An excel file programming these  
 128 simulations is available to downloaded.